

# Bifurcation and stability analysis in musculoskeletal systems: a study in human stance

B. W. Verdaasdonk<sup>1</sup>, H. F. J. M. Koopman<sup>1</sup>, S. A. van Gils<sup>2</sup>, F. C. T. van der Helm<sup>1</sup>

<sup>1</sup> Department of Bio-mechanical Engineering, Faculty of Engineering Technology, University of Twente, P.O. Box 217, 7500 AE, Enschede, The Netherlands

<sup>2</sup> Applied Analysis and Mathematical Physics Group, Department of Applied Mathematics, University of Twente, P.O. Box 217, 7500 AE, Enschede, The Netherlands

Received: 20 June 2003 / Accepted: 27 May 2004 / Published online: 12 August 2004

**Abstract.** Reflexes are important in the control of such daily activities as standing and walking. The goal of this study is to establish how reflexive feedback of muscle length, velocity, and force can lead to stable equilibria (i.e., posture) and limit cycles (e.g., ankle clonus and gait). The influence of stretch reflexes on the behavior and stability of musculoskeletal systems was examined using a model of human stance. We computed branches of fold and Hopf bifurcations by numerical bifurcation analysis of the model. These fold and Hopf branches divide the parameter space, constructed by the reflexive feedback gains, into regions of different behavior: unstable posture, stable posture, and stable limit cycles. These limit cycles correspond to a neural deficiency, termed ankle clonus. We also linked bifurcation analysis to known biomechanical concepts by linearizing the model: the fold branch corresponds to zero ankle stiffness and defines the minimal muscle length feedback necessary for stable posture; the Hopf branch is related to unstable reflex loops. Crossing the Hopf branch can lead to the above-mentioned stable limit cycles. The Hopf branch reduces with increasing time delays, making the subject's posture more susceptible to unstable reflex loops. This might be one of the reasons why elderly people, or those with injuries to the central nervous system, often have trouble with standing and other posture tasks. The influence of cocontraction and force feedback on the behavior of the posture model was also investigated. An increase in cocontraction leads to an increase in ankle stiffness (i.e., intrinsic muscle stiffness) and a decrease in the effective reflex loop gain. On the one hand, positive force feedback increases the ankle stiffness (i.e., intrinsic and reflexive muscle stiffness); on the other hand it makes the posture more susceptible to unstable reflex loops. For negative force feedback, the opposite is true. Finally, we calculated areas of reflex gains for perturbed stance and quiet stance in healthy subjects by fitting the model to data from the literature. The overlap of these areas of reflex gains could indicate that stretch reflexes are the

major control mechanisms in both quiet and perturbed stance.

In conclusion, this study has successfully combined bifurcation analysis with the more common biomechanical concepts and tools to determine the influence of reflexes on the stability and quality of stance. In the future, we will develop this line of research to look at rhythmic tasks, such as walking.

## 1 Introduction

For healthy people, walking seems an easy task, since for them it is an effortless and robust way of locomotion. However, people with an orthosis or prosthesis and people with a decreased capacity of the central nervous system (e.g., older people, CVA patients) often find walking difficult. They need to put more effort in each step, become tired more quickly, and are less able to deal with perturbations (e.g., a push). To help these groups, the principles that make normal walking such a robust and efficient form of locomotion must be discovered first.

If people are slightly perturbed by their environment during walking, they tend to return to their original periodic movement. This periodic orbit that gait approaches each time it is perturbed can be described by a *stable* limit cycle (e.g., Garcia et al. 1998; Hurmuzlu and Basmoglu 1994). A limit cycle is termed *stable* if the system under consideration returns to this cycle after small perturbations. The mathematical description of walking as approaching a stable limit cycle gives us the opportunity to explore the influence of physiological parameters on the qualitative behavior and stability of gait. Simplified segment models of humans show unactuated walking down a shallow slope (Garcia et al. 1998; McGeer 1989; Schwab and Wisse 2001), which McGeer termed *passive dynamic walking* (McGeer 1990). Such models can be seen as damped mechanical nonlinear oscillators, maintaining oscillation by a small supply of gravitational energy (by means of the slope), which compensates for energy losses due to friction and heel strike. It is this interaction between energy loss and energy supply that creates the limit cycle

Correspondence to: B. W. Verdaasdonk  
(e-mail: b.w.verdaasdonk@ctw.utwente.nl,  
Tel.: +31-53-4892822, Fax: +31-53-4893695)

to which the model returns after small perturbations. The drawback of passive dynamic walking is its poor robustness against perturbations. Schwab and Wisse (2001) have quantified the robustness by computation of the *basin of attraction* of the simplest walking model of Garcia et al. (1998); they showed that the basin was very small.

Humans exploit the natural dynamics of their body during walking. At a certain velocity they walk with minimum effort per unit distance traveled (Inman et al. 1981; McMahon 1984). It is this velocity people mostly adopt, exploiting natural dynamics to the maximum and resembling passive dynamic walking most closely. However, unlike the passive dynamic walking models, humans can adapt their speed (i.e., change to another limit cycle) and are robust against larger perturbations. A major contribution to this adaptability and robustness comes from reflexes and probably from central pattern generators. The functional role of muscle, load receptor (probably Golgi tendon organs), and cutaneous reflexes in gait is discussed in depth by Zehr and Stein (1999). They conclude that stretch reflexes are important in, among other factors, providing stability against perturbations in the swing phase and in providing both weight support and stability in the stance phase. Load receptor reflexes could be important in the stance and stance-to-swing phase and affect the period of the limit cycle, although it is unclear to what extent. To fulfill their functional role during gait, reflexes are modulated (i.e., phase dependent), but the mechanisms that cause this modulation are not yet known precisely. A central pattern generator (CPG) could play an important part in the phase modulation of reflexes during walking. A CPG is a neural oscillator that entrains to the “mechanical oscillator” (i.e., segment model), thus providing an activation pattern that in turn leads to stable locomotion. Evidence for the existence of CPGs were found, for example, in lampreys (Cohen and Wallen 1980; Grillner et al. 1981) and cats (Amemiya and Yamaguchi 1984; Brown 1911; Shik et al. 1966). Although there is no direct evidence of CPGs in humans, there is a growing number of observations suggesting their presence in the human spine (reviews by Duysens and Van de Crommert 1998; MacKay-Lyons 2002). Taga (1995a,b, 1998) and Taga et al. (1991) have successfully used simple CPGs in their neuromusculoskeletal models of human locomotion in order to achieve robust locomotion.

In this paper, we investigate the qualitative influence of reflexes on the behavior and stability of musculoskeletal systems. The goal is to establish how reflexive feedback of muscle lengthening, velocity and force, and the time delays, present in these reflex arcs, can lead to stable equilibria (i.e., posture) and limit cycles (e.g., ankle clonus, gait). As reflex gains or time delays are varied, changes may occur in the qualitative structure of the solutions to the delayed differential equations that describe the model. These changes are termed *bifurcations* and may reveal significant behavior of the musculoskeletal system. This study considers stance (i.e., posture) but also provides a framework for future research into the influence of certain types of reflexes on the behavior and stability of physiologically based gait models.

In the next section, the model is outlined. It is a model of stance, consisting of an inverted pendulum with an antagonistic muscle pair around the ankle joint and reflexive feedback of muscle lengthening, velocity, and force. The model is complex enough to demonstrate some basic influences of reflexes on the qualitative behavior of musculoskeletal systems. Necessary conditions for stable and unstable equilibria to become stable limit cycles are discussed and mathematical concepts from the bifurcation analysis are linked to known biomechanical concepts such as stiffness. The influence of reflex gains, delays, and cocontraction on the qualitative behavior of the model is investigated by using bifurcation analysis. Finally, the model is fitted to data of perturbed and quiet stance.

## 2 Methods

### 2.1 Musculoskeletal model of stance

A simple posture model is used to investigate the influence of reflex gains, delays, and cocontraction on the qualitative behavior and stability of musculoskeletal systems. The model consists of an inverted pendulum with an antagonistic muscle pair, as shown in Fig. 1. The inverted pendulum represents a person who tries to maintain an upright position by flexing and extending the ankles. Stance is assumed to be a perturbed equilibrium (e.g., by measurement errors of muscle spindles), thus producing sway. The only joint in this model represents the ankle joints, and the two muscles represent the tibialis anterior muscle and the soleus muscle for both legs. The lumped Hill-type muscle model is based on the work of Winters and Stark (1985, 1987) and models both activation and contraction dynamics. It consists of a contractile element (CE) and a serial elastic element (SE), which is modeled as nonlinear spring. The frequently used parallel elastic element has been omitted because it has no influence on the local stability of the considered posture (i.e., eigenvalues). Two types of feedback are incorporated into the model: intrinsic feedback (force-length and force-velocity relationships of the muscle) and reflexive feedback. This feedback defines the viscoelastic properties of the muscle pair.

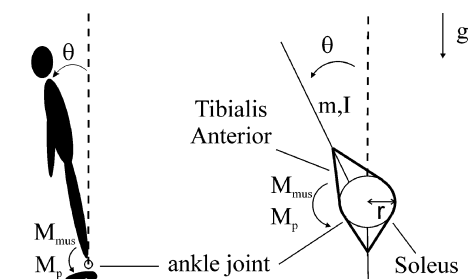


**Fig. 1.** Simplified human posture (*left*) and dynamic model representation as inverted pendulum with muscles (*right*). Parameters are mass  $m$ , moment of inertia  $I$ , moment arm  $r$ . The muscle moment  $M_{\text{mus}}$  tries to keep the angle  $\theta$  to a minimum despite the destabilizing actions of the perturbation moment  $M_p$  and gravity  $g$

The equation of motion for the inverse pendulum with mass  $m$ , moment of inertia around the ankles  $I$ , distance from ankles to center of mass  $l_{\text{com}}$ , and gravitational constant  $g$  are written as

$$I \ddot{\theta} = m g l_{\text{com}} \sin \theta + M_{\text{mus}} + M_p \quad (1)$$

in which  $\theta$  is the angle of the pendulum with respect to the vertical position,  $M_{\text{mus}}$  is the moment around the ankles produced by the muscle forces  $\mathbf{F}_{\text{mus}}$  via their constant moment arms  $r$ , and  $M_p$  is the perturbation moment imposed by the environment. The activation and contraction dynamics of the Hill-type muscles are presented in (2) and (3), respectively. Both muscles are parameterized as a soleus muscle (Thunnissen 1993; Yamaguchi et al. 1990) for simplicity (i.e., symmetric model):

$$\dot{\mathbf{a}} = f_a(\mathbf{a}, \mathbf{u}, \Delta \mathbf{l}_{\text{mus}}(t - \tau), \mathbf{v}_{\text{mus}}(t - \tau), \mathbf{F}_{\text{mus}}(t - \tau), k_p, k_v, k_f), \quad (2)$$

$$\dot{\mathbf{l}}_{\text{ce}} = f_c(\mathbf{Fv}_{\text{ce}}(\mathbf{a}, \mathbf{Fl}_{\text{ce}}, \mathbf{F}_{\text{se}})). \quad (3)$$

Equation (2) is a delay differential equation (DDE). The dependence on time  $t$  is only written explicitly in case of a delay because otherwise the equations could be mistaken to be nonautonomous. The vector  $\mathbf{a}$  represents the active states of both muscles, and  $\mathbf{u}$  is the neural input vector. The vectors  $\Delta \mathbf{l}_{\text{mus}}$  and  $\mathbf{v}_{\text{mus}}$  represent the muscle lengths (relative to the rest lengths) and the muscle velocities, respectively. They are fed back by the reflexive gains  $k_p$  and  $k_v$ , respectively, with a time delay  $\tau$ . This feedback of muscle lengths and velocities represents the stretch reflexes and reciprocal inhibition found in all antagonistic muscle pairs. Force feedback by Golgi tendon organs is represented by an ipsilateral feedback of each muscle force by a reflex gain  $k_f$ , with time delay  $\tau$ .

Equation (3) is an inverse force–velocity relationship. The vector  $\mathbf{Fv}_{\text{ce}}(\mathbf{a}, \mathbf{Fl}_{\text{ce}}, \mathbf{F}_{\text{se}})$  represents the momentary values of the force–velocity relationships of the CEs of both muscles, which is obtained by recognizing that the force in the SE must be equal to the force in the CE in this muscle model. These force–velocity relationships are expressed in terms of the momentary values of the force–length relationships of the CEs  $\mathbf{Fl}_{\text{ce}}$  and the forces in the SEs  $\mathbf{F}_{\text{se}}$ . The elaborate form of (1), (2), and (3) is found in Appendix A.

The model contains a total of six state variables: the angle  $\theta$ , the angular velocity  $\omega$ , the active states of the tibialis anterior and the soleus,  $a_{\text{ta}}$  and  $a_{\text{sol}}$ , and the lengths of the CEs of both muscles,  $l_{\text{ce,ta}}$  and  $l_{\text{ce,sol}}$ . However, because of reflexive feedback, the angle and angular velocity also appear in delayed form,  $\theta(t - \tau)$  and  $\omega(t - \tau)$ , respectively. Thus, the system is of infinite order. The considered equilibrium is standing upright, which corresponds to zero angle, zero angular velocity, and for both muscles constant, equal, active states and lengths of the CEs. The muscles have different time constants for increasing and decreasing muscle activation, and there is a discontinuity in the slope of force–velocity curve of the CEs at zero velocity. These discontinuities are exactly in the equilibrium and render bifurcation analysis difficult. Therefore, they have been approximated with the help of a “sharp”

tangent hyperbolic function (i.e., steep slope), as shown in Appendix B. Numerical simulations showed no significant change in behavior between the model with real discontinuities and the one with the smoothed discontinuities.

## 2.2 Bifurcation analysis

The purpose of the performed bifurcation analysis is to identify the influence of those parameters that can be adjusted by the central nervous system. These are assumed to be the supraspinal neural input vector  $\mathbf{u}$  and the reflexive feedback gains of the muscle length, velocity, and force,  $k_p$ ,  $k_v$ , and  $k_f$ , respectively. The neural input for both muscles is assumed to be equal, thus  $\mathbf{u} = [u_{\text{ta}} \ u_{\text{sol}}]^T = [u \ u]^T$ . The influence of a time delay  $\tau$ , inevitably present in all reflex arcs, is also analyzed. Time delays limit the maximum reflex gains possible for a stable posture, as is known from control engineering. However, the influence of time delays on the occurrence and stability of limit cycles is less clear.

A bifurcation is the appearance of a topologically nonequivalent phase portrait under parameter variation (Kuznetsov 1998). Local bifurcations of a continuous time system, to which we confine ourselves in this paper, may occur when eigenvalues of the linearization about an equilibrium pass the imaginary axis as parameters vary. The two most common bifurcations for such systems are the fold and the Hopf bifurcation, which are conventional textbook paradigms (e.g., Arrowsmith and Place 1990; Iooss and Joseph 1990; Seydel 1988). The *fold* bifurcation is associated with the appearance or disappearance of two equilibria. In symmetric systems, such as the musculoskeletal model, the fold bifurcation often manifests itself as a *pitchfork* bifurcation (Kuznetsov 1998). Beyond this type of fold bifurcation, an additional third equilibrium is present, which changes stability at the bifurcation point (eigenvalue of the considered equilibrium passes through zero with nonzero speed). It is this type of fold bifurcation that is associated with the stability of posture in the musculoskeletal model, with the third equilibrium representing the posture. A *Hopf* bifurcation occurs when a conjugated pair of eigenvalues passes the imaginary axis with nonzero speed. The Andronov–Hopf theorem gives conditions that guarantee that a limit cycle will appear or disappear after a Hopf bifurcation (Arrowsmith and Place 1990). Note that there are two different scenarios, namely, the subcritical and the supercritical Hopf bifurcation, but only the latter leads to stable limit cycles. The local stability of encountered limit cycles can be assessed by placing a (hyper) surface transverse to the flow near the limit cycle. The crossings of the orbit with this surface in a given direction can be seen as a discrete representation of the flow near the limit cycle. This discrete map is called a Poincaré map – or first return map – and has a state space whose dimension is reduced by one relative to the original continuous time system. The limit cycle is represented by a *fixed point* (i.e., rest point) of the Poincaré map. The limit cycle will be locally stable if the fixed point of the Poincaré map is locally stable. This is determined by calculating the eigenvalues of the Poincaré

map, which are called *Floquet multipliers*. All multipliers have to be within the unit circle (i.e., in absolute value smaller than 1) for the limit cycle to be locally asymptotically stable (Kuznetsov 1998).

Stretch reflexes (position and velocity feedback) are generally known to have an important regulatory function in posture as well as in locomotion (Houk 1979). Cocontraction is an effective – but also very energy-consuming – way of regulating the viscoelastic properties of muscles and is probably only used when necessary. Therefore, our analysis starts by looking at the influence of the stretch reflex at a low cocontraction level. A parameter space is constructed with the positional gain  $k_p$  on the horizontal axis and the velocity gain  $k_v$  on the vertical axis. In such a space, the dependence of existing bifurcations on those parameters can be shown. The functional role of force feedback is less clear and will be analyzed subsequently in the same parameter space. The steps of the analysis are described in the paragraph below.

First, the equilibria of the DDEs [(1), (2), and (3)] are calculated for a reference set of parameters. At these equilibria, the system is linearized and, at least, the rightmost eigenvalues – that is, the eigenvalues with the largest real parts (Lyapunov exponents) – have to be calculated, because these play a dominant role in the system's behavior and stability. Second, one of the parameters is changed so that the rightmost eigenvalues cross the imaginary axis. If it concerns a single eigenvalue with zero imaginary part, a fold bifurcation is encountered, whereas if it concerns a conjugated pair of eigenvalues, a Hopf bifurcation has occurred. From a fold point a whole branch of fold points can be followed through parameter space spanned by  $k_p$  and  $k_v$ . Similarly, from a Hopf point a branch of Hopf points can be computed, which is represented by a set of combinations of  $k_p$  and  $k_v$ .

The calculated fold and Hopf branches, with the reflex gains  $k_p$  and  $k_v$  as parameters, will be used as reference branches for determination of the influence of the other parameters. The influence of time delay  $\tau$ , equal neural inputs  $u$  (level of cocontraction), and force feedback gain  $k_f$  will be determined by calculation of the fold and Hopf branches in the same parameter space, in the same way as described above. Only the parameter whose influence is to be determined is changed relative to the reference parameter set. The influence of those deviating parameters can be observed by comparing the reference bifurcation branches with the ones with deviating parameter sets. Choosing the same parameter space, instead of constructing new ones with the deviating parameter on one of the axis, is important since it allows the influence of parameters to be compared.

The intersections of fold and Hopf branches can lead to mathematically intriguing bifurcation points, such as the Bogdanov–Takens bifurcation and the fold–Hopf bifurcation (Kuznetsov 1998). These bifurcations were indeed encountered in the analysis (Sect. 3.1) but are only discussed as far as is considered relevant. It is not within the scope of this paper to review all possible behaviors in the neighborhood of such points. More significant is the subdivision of parameter space by fold and Hopf branches.

This leads to different regions in parameter space, each representing a different qualitative behavior of the model.

In analyzing musculoskeletal models, the delays present in the reflex arcs result in delayed differential equations (DDEs). The state space for a DDE is infinite dimensional. The DDE-BIFTOOL Matlab package (Engelborghs et al. 2001) is used to perform bifurcation analysis for the DDEs. This package approximates the most dominant eigenvalues, which allows the user to determine the type of bifurcation. Subsequently, DDE-BIFTOOL tests the necessary conditions for the bifurcation to be generic. The Floquet multipliers of limit cycles, emerging beyond the Hopf branch, are numerically calculated by DDE-BIFTOOL by time integration of the variational equation around the periodic solution (for details, please see Engelborghs et al. 2001).

### 2.3 Biomechanical interpretation of fold and Hopf bifurcations by linearization of the stance model

Bifurcation analysis is relatively unknown in the field of biomechanics, whereas it can be of great assistance in understanding the influence of certain parameters on the behavior and stability of biological systems. In the previous subsection (Sect. 2.2), fold and Hopf bifurcations were discussed. In this section, a linearized model is constructed in the form of a block diagram, which makes it possible to link the fold and Hopf bifurcations to some well-known biomechanical and control engineering concepts. The musculoskeletal model (Sect. 2.1) is linearized in its equilibrium, which represents stance. The equilibrium states are entirely determined by the level of cocontraction  $a_{co}$ . The active states of the muscles in equilibrium are equal to the level of cocontraction ( $a_{ta} = a_{sol} = a_{co}$ ), and cocontraction also determines the length of the contractile elements (CE),  $l_{ce,ta}$ , and  $l_{ce,sol}$ . Higher cocontraction leads to a decreased length of the CEs such that a new force equilibrium with the SEs is established, with higher force and generally higher muscle stiffness and viscosity. The angle  $\theta$  and angular velocity  $\omega$  are both zero in the equilibrium because both muscles have the same rest length and neural input  $u$ . The level of cocontraction is mainly determined by the neural input but can also be increased or decreased by force feedback. Positive force feedback will increase the level of cocontraction, while negative force feedback will decrease it. Feedback of the muscle lengths and velocities does *not* change the level of cocontraction  $a_{co}$ . The stability of the equilibrium depends on the level of cocontraction and on the reflexive feedback of muscle lengths, velocities, and forces. The feedback of muscle lengths and velocities is proven to be especially important in keeping the posture stable (Van der Helm et al. 2002). Time delays in these reflex arcs limit the maximum possible feedback gains because the gain and phase margin of the reflex loop is decreased by the extra phase lag introduced by time delays. In other words, time delays jeopardize the stability of the posture at high reflex gains.

The linearized model is shown in Fig. 2. The scheme is similar to the linearized musculoskeletal models used

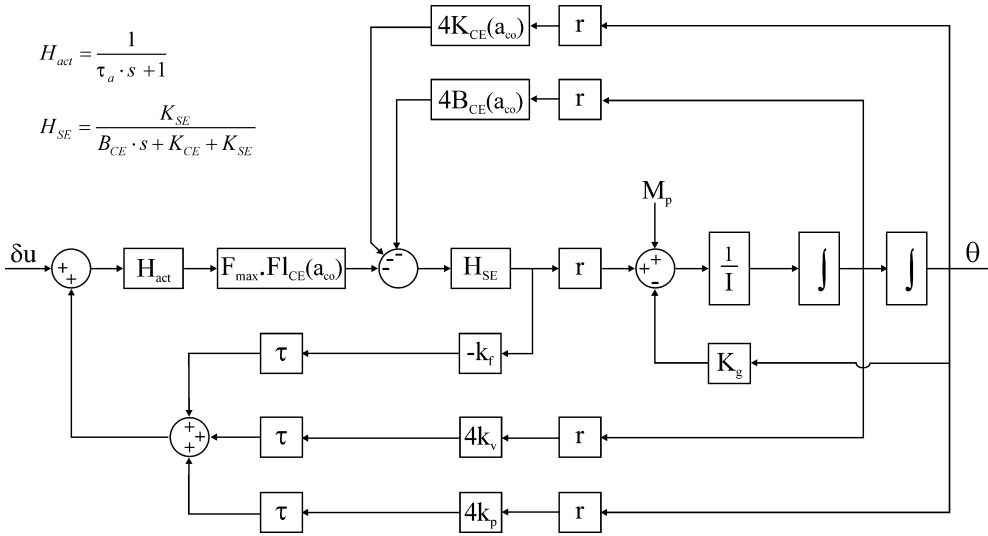


**Fig. 2.** Linearized model of the musculoskeletal system including intrinsic viscoelastic properties of the muscles ( $K_{CE}$  is stiffness of CE,  $B_{CE}$  is viscosity of CE, and  $H_{SE}$  is viscoelastic properties due to SE) and delayed reflexive feedback of muscle length, velocity, and force with gains  $k_p$ ,  $k_v$ , and  $k_f$ , respectively. The delay  $\tau$  is modeled by a Padé approximation. Segment model parameters are moment

of inertia  $I$ , moment arm  $r$ , and gravitational stiffness  $K_g$ . Muscle parameters are maximal force  $F_{max}$  and the value of the force-length relationship in equilibrium  $Fl_{CE}(a_{co})$ .  $H_{act}$  represents the muscle activation dynamics. Inputs are neural input fluctuations  $\delta u$  and perturbation moment  $M_p$ . Output is angle of inverse pendulum relative to vertical  $\theta$

by van der Helm and Rozendaal for analyzing shoulder posture tasks (Van der Helm and Rozendaal 2000). However, in our model the influence of the SEs of the muscles is not discarded because the soleus and tibialis anterior have long tendons. Therefore, the SEs of the modeled muscles are compliant (relative to, for example, shoulder muscles) and have a large influence on the behavior and stability of the posture. In the linearized model, this influence is represented by the transfer function  $H_{SE}$ . This is recognized as the viscoelastic behavior of the SE in series with the CE. In most muscles of the upper extremity, the SE is very stiff because the tendons are relatively short. In such cases, the influence of the SE in the muscle model can be neglected, but this is generally not true for muscles in the lower extremities.

Gravity has a destabilizing effect on the posture of the inverted pendulum and is modeled as a negative stiffness. This negative gravitational stiffness  $K_g = -mgl_{com}$  must be compensated by intrinsic and reflexive feedback so as to achieve a stable posture.

Intrinsic feedback is achieved by cocontraction  $a_{co}$ . This cocontraction results in a certain stiffness  $K_{CE}$  and viscosity  $B_{CE}$  of the CE of each muscle. The stiffness  $K_{CE}$  of the muscle model is proportional to the cocontraction and the derivative of the force-length relationship at the equilibrium length of the CE. The viscosity  $B_{CE}$  of the muscle model is proportional to the cocontraction, the force-length relationship at the equilibrium length of the CE, and the derivative of the force-velocity relationship at zero velocity of the CE. As the length of the CEs is determined by the cocontraction,  $K_{CE}$  and  $B_{CE}$  only depend on the level of cocontraction.

Reflexive feedback is achieved by feedback of muscle length, velocity, and force with gains  $k_p$ ,  $k_v$ , and  $k_f$  respectively. All reflexive feedback is proportional to the value of

the force-length relationship in the equilibrium  $Fl_{ce}(a_{co})$ , as shown in the block diagram. The time delay  $\tau$  is modeled as a third-order Padé approximation (Appendix C) in the linearized block diagram, which gives good results, predicting the eigenvalues of the model (at least up to the transition from linear stability to linear instability). The stretch reflex is modeled as the feedback of angle  $\theta$  and angular velocity  $\omega$  because these are directly related to muscle length and velocity (Appendix A). Ideally, the feedback of muscle length would purely define muscle stiffness and the feedback of muscle velocity would purely define muscle viscosity. However, the activation dynamics  $H_{act}$ , viscoelastic dynamics  $H_{SE}$ , and especially the delay  $\tau$  ( $H_\tau = e^{-j\omega\tau}$ ) add a considerable phase lag to the reflex loop, endangering the stability of posture. The viscoelastic dynamic properties due to the SE,  $H_{SE}$ , not only introduces phase lag but also reduces the total muscle stiffness. It becomes  $K_{mus} = \frac{K_{SE}(K_{CE} + K_R)}{K_{SE} + K_{CE}}$ , with  $K_{SE}$  the stiffness of the SE,  $K_{CE}$  the intrinsic stiffness of the CE, and  $K_R$  the reflexive contribution to the stiffness of the CE.

The contribution of force feedback with gain  $k_f$  is two-fold. First, as mentioned above, force feedback changes the level of cocontraction  $a_{co}$ . Positive force feedback will increase the cocontraction and thereby increase the intrinsic and reflexive contributions to muscle stiffness and viscosity. Negative force feedback will decrease the muscle stiffness and viscosity. Second, force feedback introduces some extra dynamics because it modulates the intrinsic and reflexive feedback loops, as shown in the block diagram (Fig. 2). Positive force feedback makes activation dynamics become more dominant, giving more phase lag at low frequencies. This leads to linear instability if this phase lag is not compensated by additional feedback of muscle velocity. On the other hand, negative force feedback will decrease the intrinsic and

reflexive contributions to muscle stiffness and viscosity. The activation dynamics become less dominant, giving less phase lag at low frequencies in the reflexive loops, and the posture might therefore be less susceptible to instability.

It has long been known that negative force feedback exists in humans (Sherwood 1997), and at one time it was thought that its sole purpose was the protection of muscles from overload. Later, the functions of stiffness regulation (Houk 1979) and compensation for muscle fatigue (Kirsch and Rymer 1987) were hypothesized. The existence of positive force feedback in humans is still the subject of debate (Capaday 2000, 2001; Duysens 2000). The exact role of force feedback in posture and locomotion is not yet clear, although it does seem to be significant (Dietz 1998; Dietz and Duysens 2000; Duysens et al. 2000).

The linearized model of stance can predict the eigenvalues of the posture quite well. Therefore, it will be used to provide insight into the physical causes of encountered fold and Hopf bifurcations (Sects. 3.1–3.4). A limitation of the linearized model is that the behavior will only be correctly predicted if the posture is stable and the perturbations are small. Hence, bifurcation analysis is necessary to predict the behavior of the posture when it has become linearly unstable.

### 3 Results of the numerical simulations

In this section, the influence of stretch reflexes (including reciprocal inhibition), time delays, cocontraction, and force feedback on the behavior of the musculoskeletal model of stance is discussed. Stability regions of posture and periodic movement in parameter space ( $k_p$  vs.  $k_v$ , Sect. 2.2) will be distinguished with the help of bifurcation analysis. The linearized model described in Sect. 2.3 will be used to link these findings with known concepts in the biomechanical field. Section 3.5 describes how the model is fitted to data from literature about quiet and perturbed stance in order to get a notion of normal feedback gains in healthy people.

To begin our analysis, a reference parameter set has to be chosen. This defines the reference equilibrium in state space and accompanying eigenvalues. The reference parameter set is  $[u \ k_p \ k_v \ k_f \ \tau]^T = [0.1 \ 50 \ 10 \ 0 \ 50e-3]^T$ , where  $u$  is the value of both neural inputs,  $k_p$ ,  $k_v$ , and  $k_f$  are the reflexive feedback gains of the muscle lengthening, velocity, and force, respectively, and  $\tau$  is the time delay present in the reflex arcs. A low level of neural input ( $u = 0.1$ ) is chosen, which is not enough to stabilize the posture without reflexive feedback. The influence of stretch reflexes is studied first, and thus the force feedback gain  $k_f$  is initially set to zero. The reference gains  $k_p = 50$  and  $k_v = 10$  stabilize the posture. A reference delay  $\tau$  of 50 ms is chosen because this is typical for the short latency reflexes found in human ankle flexors and extensors (Sinkjaer et al. 1988). These parameters give an equilibrium at

$$\mathbf{x}_{\text{eq,ref}} = [a_{\text{ta}} \ a_{\text{sol}} \ l_{\text{ce,ta}} \ l_{\text{ce,sol}} \ \theta \ \omega]^T = [0.1 \ 0.1 \ 0.936 \ 0.936 \ 0 \ 0]^T,$$

with accompanying rightmost eigenvalues  $\lambda_{\text{rm,ref}} = -1.46 \pm 4.54j$  (i.e., posture is stable). As mentioned in

Sect. 2.3, the states of the equilibrium  $\mathbf{x}_{\text{eq}}$  only depend on the value of the neural inputs  $u$  and on the force feedback gain  $k_f$ . However, the stability of the equilibrium also depends on the positional feedback gain  $k_p$ , the velocity feedback gain  $k_v$ , and the delay  $\tau$  of the reflex arc.

#### 3.1 Influence of stretch reflexes on model behavior and stability

The influence of stretch reflex gains on the behavior of the model is explored by looking at bifurcations in parameter space, with the positional gain  $k_p$  on one axis and the velocity gain  $k_v$  on the other. A bifurcation point is found by varying one parameter while looking at the rightmost eigenvalues of the equilibrium because they dominate the system behavior. Figure 3 shows the real part of the rightmost eigenvalues  $\lambda_{\text{rm}}$  in dependence on  $k_p$ , while the other parameters are kept constant at their reference value.

The events for which the rightmost eigenvalues go through the imaginary axis are marked in the figure by circles, and these correspond to a fold and a Hopf bifurcation. Distinguishing between a Hopf and a fold bifurcation from this figure is not possible. However, looking at the imaginary part of the eigenvalues will reveal the nature of the bifurcation (Sect. 2.2).

A fold and a Hopf branch are continued in parameter space, with the previously determined bifurcation points as starting points. Figure 4 shows the fold and the Hopf branch as well as the starting points. The fold branch is a vertical line, indicating that the fold bifurcation only depends on  $k_p$ .

The fold and Hopf branches divide parameter space into four regions, marked I, II, III, and IV in the figure. The intrinsic stiffness of the muscles, induced by a cocontraction of 10%, is too small to compensate for the negative stiffness caused by the gravitational force. Thus, without reflexive feedback ( $[k_p, k_v] = [0, 0]$  in the figure) the pendulum will fall to  $\pm\pi$  because the muscles have no parallel element. Reflexive feedback of the muscle length-

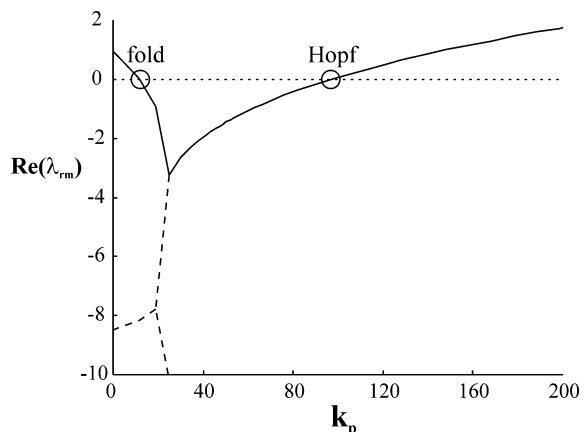


**Fig. 3.** The real part of the rightmost eigenvalues versus the positional feedback gain  $k_p$ . The other parameters are kept constant at reference values. The *left marking* represents a fold bifurcation (one eigenvalue through zero), the *right marking* represents a Hopf bifurcation (conjugated pair of eigenvalues through imaginary axis)

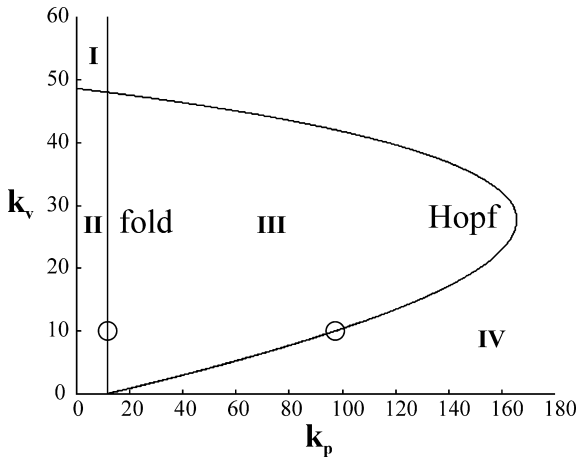


**Fig. 4.** Hopf and fold bifurcations in parameter space. The parameters are the positional feedback gain  $k_p$  and the velocity feedback gain  $k_v$ . The starting points of the bifurcation branches are marked and correspond to the marked points in Fig. 3. The fold and Hopf branch divide the parameter space in four different regions: I, II, III, IV. In regions I and II the posture is unstable and the person will “fall”. The posture is stable in region III, and in region IV oscillatory movements are experienced (i.e., limit cycles)

ening will increase the muscle stiffness. For a given level of cocontraction, a certain minimal positional feedback gain  $k_{p,\min}$  is necessary in order to compensate for the negative “gravitational stiffness”  $K_g$ . This minimal feedback gain of the muscle length,  $k_{p,\min}$ , is represented by the vertical fold bifurcation line in the figure. Thus, in regions I and II the person falls because the total ankle stiffness, caused by muscles and gravity, is negative.

For stable posture, besides the minimal positional feedback gain  $k_{p,\min}$ , a minimal velocity feedback gain  $k_{v,\min}$  is also necessary. Velocity feedback is necessary to compensate for the phase lag caused by time delay in the reflex arcs, muscle activation dynamics, and the presence of a compliant SE (Sect. 2.3). Figure 5 shows the minimal feedback gains to be  $[k_{p,\min}, k_{v,\min}] = [11.7, 5.5e-2]$ . This point is an intersection of the fold and Hopf branch and has a double zero as rightmost eigenvalues. It is, in fact, a Bogdanov–Takens (BT) bifurcation and it is the start of the Hopf branch in parameter space.

The lower part of the Hopf branch (Fig. 4), up to the turn ( $[k_p, k_v] = [165.6, 27.6]$ ), represents all possible positional feedback gains  $k_p$  with accompanying minimal velocity feedback gains  $k_v$ . For higher velocity gains, the posture is stable; for lower gains it is unstable. However, if velocity gains increase too much, the reflex loop also becomes unstable. The upper part of the Hopf branch is associated with these maximal velocity feedback gains. To the right of the turning point of the Hopf branch the posture is also unstable because the positional feedback is too high for any velocity feedback. Thus, in region III the posture is stable because the lack of intrinsic stiffness is compensated by a large enough positional feedback. In addition, the phase lag, introduced mostly by time delay, is compensated by a velocity feedback.

If one travels from region III to IV across the Hopf branch, the phase and/or gain margin reduces and the stability of the posture vanishes. Instead, a limit cycle

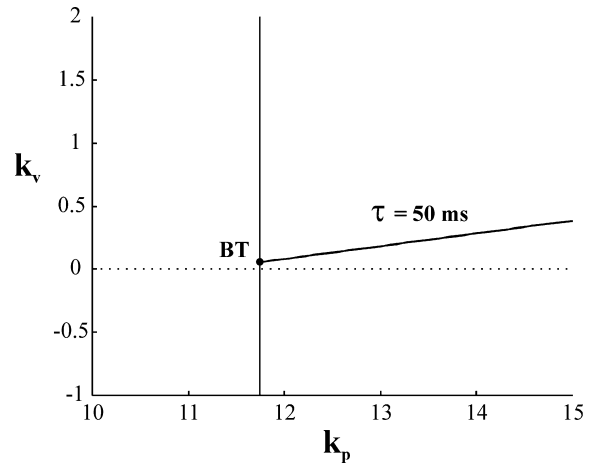


**Fig. 5.** Zoom-in of Fig. 4. BT is a Bogdanov–Takens bifurcation, the first intersection of fold and Hopf branch and representing the minimal feedback gains  $[k_{p,\min}, k_{v,\min}] = [11.7, 5.5e-2]$  above which the posture will be stable (up to certain maximum gains)

originates around the equilibrium states of the previously stable posture. Limit cycles can only exist for nonlinear systems, and their local stability is determined by the eigenvalues of the Poincaré map (i.e., linearization about the cycle), called Floquet multipliers (Sect. 2.2). The Floquet multipliers of the limit cycles were calculated and the absolute values were always less than unity, indicating stable limit cycles just beyond the Hopf branch in all of region IV. In Fig. 6, the size of the imaginary part of the conjugated pair of eigenvalues associated with the Hopf bifurcation is shown. The size of the imaginary part  $Im$  is directly related to the period  $T$  of the sinusoidal periodic solutions just beyond these Hopf points ( $T = 2\pi/Im$ ).

Along the Hopf branch, for increasing velocity gain  $k_v$ ,  $Im$  increases (i.e.,  $T$  decreases) from 0 [rad/s] at the BT to 16.0 [rad/s] at the second intersection of the fold and Hopf branch. This intersection has a zero and a conjugated pair of eigenvalues on the imaginary axis and is in fact a fold–

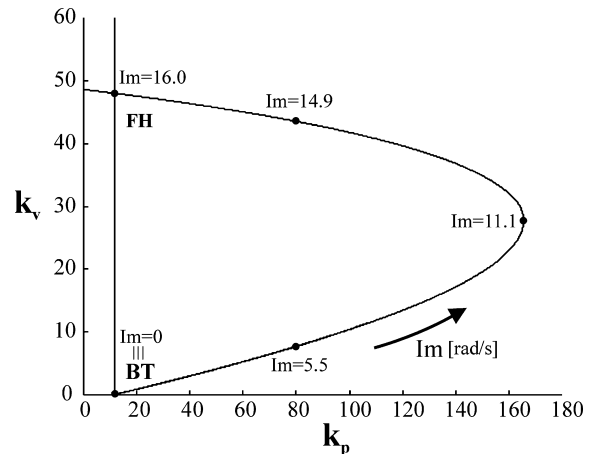


**Fig. 6.** Size of imaginary parts  $Im$  of conjugated pair of eigenvalues related to the Hopf bifurcations plotted along the Hopf branch. The period  $T$  of limit cycles just beyond these Hopf points is about  $T = 2\pi/Im$

Hopf (FH) bifurcation. Left from the FH, in region I, the limit cycles are unstable. In the neighborhood of the BT and FH bifurcations, complex dynamical behavior can be expected, such as homoclinic cycles (BT) and tori (FH). However, analysis of these complex behaviors is not within the scope of this paper. See Kuznetsov (1998) for more information about BT and FH bifurcations and about the possible system behavior in their neighborhoods.

The observed limit cycles do *not* represent the sway experienced during stance, because sway is assumed to be the result of perturbations acting on a stable equilibrium (Sect. 2.1). They are more likely to be related to a pathological case termed ankle clonus. Clonus is a sustained rhythmical contraction of muscles that occurs after a sudden stretch and is often caused by injury to the central nervous system. Hidler and Rymer (1999, 2000) showed that the presence of two conditions leads to clonus, namely, the presence of significant delays in the reflex paths and an increase in effective reflex gains, caused by a reduced motoneuron firing threshold. The ankle is one of the most distal joints, which means that there are large time delays in its reflex arcs. This is why ankle clonus is a quite common type of clonus.

The limit cycles to the right and above the Hopf branch (Figs. 4 and 6) are caused by similar mechanisms to those causing ankle clonus, namely, high reflex gains in combination with a considerable time delay in the reflex arcs. The period of the oscillations, associated with ankle clonus, depends on the feedback gains of muscle lengthening and velocity and varies between 1.8 and 2.5 Hz (Fig. 6). In the literature, frequencies of about 3–8 Hz are reported, but these are usually assessed when the patient is seated. It is therefore not surprising that our simulated frequencies, assessed using a model of stance, are somewhat lower (the moment of inertia about the ankles is much larger in stance compared to sitting).

### 3.2 Influence of reflex delay on model behavior and stability

The influence of time delay  $\tau$  on the behavior of the posture model is shown in Fig. 7 in parameter space. The fold branch does not change for different delays because it represents the muscle length feedback  $k_{p,\min}$  for zero ankle stiffness, and stiffness is defined at zero frequency. Time delay only adds phase lag proportional to frequency ( $H_\tau = e^{-j\omega\tau}$ ) and has no influence on stiffness and therefore none on the location of the fold bifurcation in parameter space either. However, time delay has a tremendous influence on the Hopf branch. For increasing delay, the Hopf branch “shrinks” because it becomes harder to compensate for the extra phase lag introduced by this delay. This causes the region of reflex gains for which the posture is stable (region III in Fig. 4) to become smaller.

The period of the stable limit cycles, emerging beyond the Hopf branch, will increase with increasing time delay. The frequency of stable oscillations is up to 6.3 Hz for zero time delay, up to 2.5 Hz for 50 ms time delay (as mentioned in the previous section), up to 1.7 Hz for 100 ms time delay,

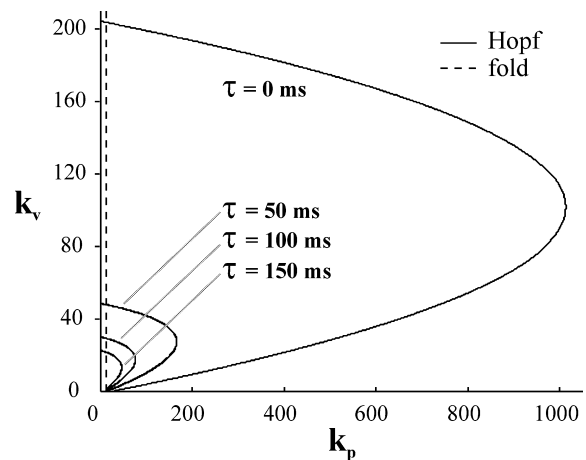


**Fig. 7.** Influence of time delays  $\tau$  on fold and Hopf branches. Fold bifurcation branch is unaffected by delay. Hopf bifurcation branch shrinks with increasing delay

and up to 1.2 Hz for 150 ms time delay. These maximum frequencies lie in the neighborhood of the FH.

Figure 8 shows a zoom-in of parameter space at the BT point. The minimal velocity feedback gain  $k_{v,\min}$  necessary for stable posture increases for increasing time delay  $\tau$  because the extra phase lag of the time delay has to be compensated by extra velocity feedback. The figure also shows that without time delay no velocity feedback would be necessary at all to obtain stable posture (although it still might give better transient response).

### 3.3 Influence of cocontraction on model behavior and stability

Increased neural input  $u$  leads to increased cocontraction  $a_{co}$  and so to shortened CE. In other words, the active states and lengths of the CEs of the muscles in equilibrium change. In Fig. 9, the influence of increased neural inputs  $u$  on the fold bifurcation in terms of positional feedback gain  $k_p$  is shown. The intrinsic stiffness of the muscles becomes greater for increasing cocontraction, and for  $u > 0.23$  the stiffness has become so great that reflexive

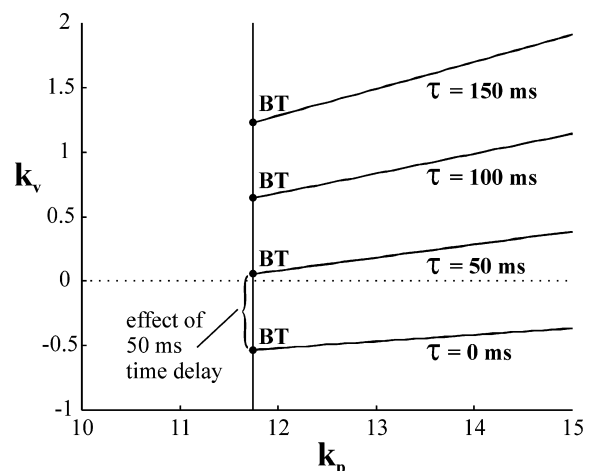


**Fig. 8.** Zoom-in of Fig. 7. Increasing time delay increases the minimal velocity feedback,  $k_{v,\min}$ , necessary for stable posture

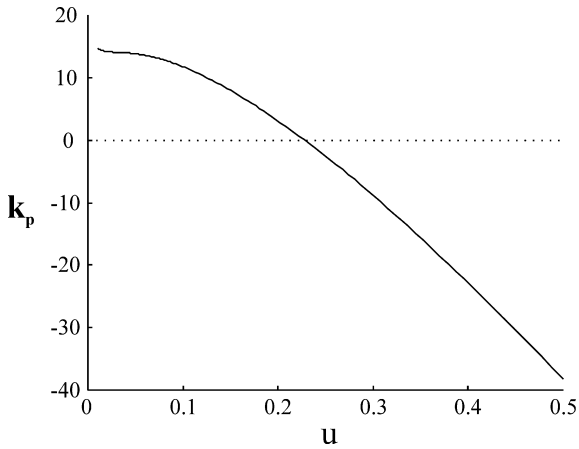


**Fig. 9.** Influence of neural input  $u$ , in this case equal to the cocontraction  $a_{co}$  (no force feedback), on fold bifurcation. The fold branch represents the minimal muscle length feedback  $k_{p,min}$  that exactly compensates for the negative gravitational stiffness: the total ankle stiffness is zero. Higher cocontraction increases the intrinsic muscle stiffness, and therefore less muscle length feedback is necessary for stable posture. For neural inputs higher than 0.23 (23% of maximal cocontraction) the posture is stable without any reflexive feedback at all

feedback is no longer necessary for stable posture ( $k_p < 0$  for  $u > 0.23$  in Fig. 9). In a parameter space of  $k_p$  versus  $k_v$  (as in Fig. 4), this would manifest itself as a shift of the vertical fold branch to the left for increasing  $u$ .

The influence of increased neural input  $u$  on the Hopf branch is shown in Fig. 10. This figure shows that the Hopf branch grows rapidly with increasing cocontraction and thus provides stable posture for much larger feedback gains. A large part of this growth is due to the fact that for increasing cocontraction the muscles will work on a lower part of their force-length relationship (below optimum length), thereby decreasing the effective reflex loop gain. Moreover, increasing the intrinsic stiffness of the muscles decreases the loop gain further, especially at low frequencies.

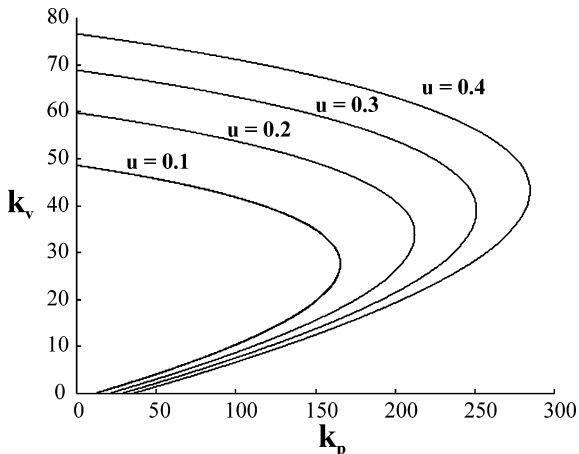


**Fig. 10.** Influence of neural input  $u$ , in this case equal to the cocontraction  $a_{co}$  (no force feedback), on Hopf branches. Increased level of cocontraction lowers the effective reflex loop gain and increases the intrinsic muscle stiffness, which leads to larger Hopf branches

The period of the stable limit cycles, emerging beyond the Hopf branch, will decrease slightly with increasing cocontraction. The frequency of the stable oscillations is up to 2.5 Hz for 10% cocontraction (as mentioned in Sect. 3.1), up to 2.7 Hz for 20–30% cocontraction, and up to 2.8 Hz for 40% cocontraction.

### 3.4 Influence of force feedback on model behavior and stability

The influence of force feedback in musculoskeletal systems is still a topic of debate. Force feedback in the model of stance has two consequences: it changes the equilibrium by changing the level of cocontraction  $a_{co}$  (Sect. 3.3) and it modulates the intrinsic and reflexive feedback loops (Sect. 2.3). The solid lines in Fig. 11 show the influence of force feedback with gain  $k_f$  on the fold bifurcation (positive  $k_f$  means positive force feedback). For positive force feedback, less or no positional feedback is necessary in terms of  $k_p$  to obtain positive ankle stiffness; for negative force feedback more positional feedback is necessary. To see the modulation effect of force feedback, the neural inputs were adapted such that there was no increase in cocontraction (i.e., same equilibrium for all  $k_f$ ). This is represented by the dashed lines and shows a linear relation between  $k_p$  and  $k_f$ .

The influence of force feedback on the Hopf branch is shown in Fig. 12. The modulation effect (dashed lines) of positive force feedback makes the Hopf branch shrink considerably, which is compensated only slightly by the effect of increased cocontraction. Negative force feedback, on the other hand, enlarges the Hopf branch. To summarize, positive force feedback increases the muscle stiffness (intrinsic and reflexive), but the posture becomes

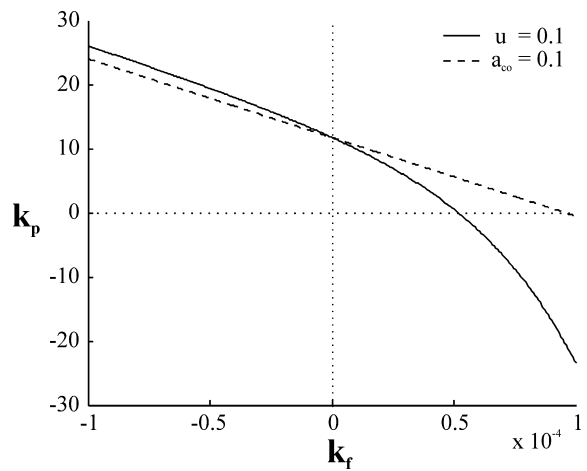


**Fig. 11.** Influence of force feedback  $k_f$  on fold bifurcation. Positive  $k_f$  means positive force feedback. *Solid lines* show influence of force feedback on fold bifurcation. Positive force feedback increases the cocontraction and modulates the intrinsic and reflexive feedback loops. This increases ankle stiffness, and therefore less muscle length feedback  $k_p$  is necessary. The effect of the modulation effect alone is shown by the *dashed lines* (cocontraction is kept constant by adapting the neural input)

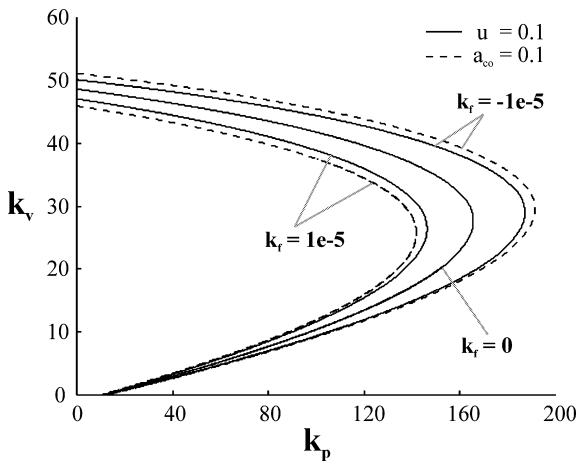


**Fig. 12.** Influence of force feedback  $k_f$  on Hopf branches. Positive  $k_f$  means positive force feedback. *Solid lines* show influence of force feedback on the Hopf branch (increased cocontraction and modulation of reflexive and intrinsic loops). The effect of the modulation effect alone is shown by the *dashed lines* (cocontraction is kept constant by adapting the neural input). The effect of modulation is dominant and causes the Hopf branch to shrink for positive force feedback

more susceptible to an unstable reflex loop. For negative force feedback, it is precisely the other way around.

The frequency of stable oscillations is not very sensitive to increasing force feedback and is up to 2.6 Hz for negative force feedback with gain  $k_f = -1e-5$  and up to 2.5 Hz for no force feedback (as mentioned in Sect. 3.1) or positive force feedback with gain  $k_f = 1e-5$ .

### 3.5 Model fit to data of quiet and perturbed stance

To get a notion about the reflex gains experienced during posture, the model was fitted to data from the literature about disturbance rejection and quiet stance in the sagittal plane. Mihelj et al. (2000) measured the effective ankle stiffness (i.e., stiffness of ankle muscles plus gravitational stiffness) in the sagittal plane in response to disturbances, relying mainly on ankle strategy (i.e., counteracting perturbations with your ankle joints only). They found it to be between 9 and 12 Nm/deg. We roughly estimated the relative damping factor at between 0.6 and 0.8 by taking the logarithmic decrement of the presented graphs. The combinations of reflex gains  $[k_p, k_v]$  reflecting these data is shown in Fig. 13 (light gray area).

Whether or not ankle stiffness – reflexive stiffness in particular – is important in quiet stance remains a topic of debate. Some believe anticipatory control makes a major contribution to stability during quiet stance (Masani et al. 2003; Morasso and Sanguineti 2002). However, Fitzpatrick et al. (1994) has shown that afferent feedback from ankle muscles is sufficient for a stable upright stance. Therefore, we fitted our model to data of quiet stance in the sagittal plane with the subject's eyes closed (Winter et al. 1998) and also plotted it in Fig. 13 (dark gray area). Figure 14 zooms in on the areas of reflex gains. The figure shows that the areas of reflex gains for perturbed stance and quiet stance overlap.

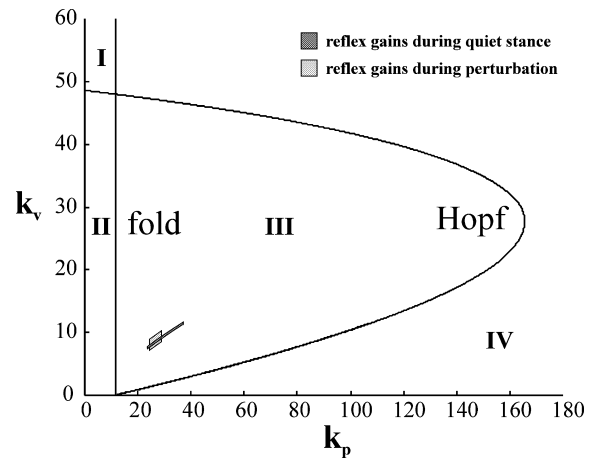


**Fig. 13.** Areas of reflex gains for the stance model fitted to data from the literature of perturbed stance (*light gray*) and quiet stance (*dark gray*)

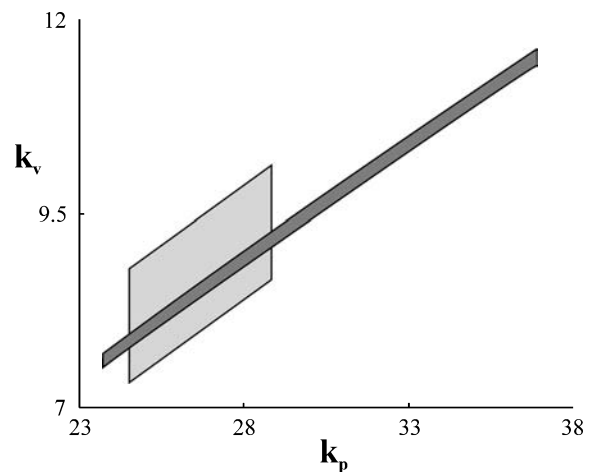


**Fig. 14.** Zoom-in of Fig. 13. The overlap of the areas of reflex gains, experienced during perturbed and quiet stance, could indicate that stretch reflexes play a major role in stabilizing the posture in both cases

Most experts agree that reflexes play a crucial role in perturbed stance. For quiet stance, it has been proposed that anticipatory control may play a key role. However, the overlap of the calculated areas of reflex gains for perturbed stance and quiet stance could be an indication that stretch reflexes are the major control mechanisms in both cases.

## 4 Discussion

### 4.1 How should stability be quantified?

The upright standing posture considered in this paper is an example of a perturbed equilibrium. Fluctuations around the equilibrium can be caused by, for example, measurement noise in muscle spindles, noise in the neural processing of the information, or environmental perturbations, such as a push. If these fluctuations are small, local asymptotic stability of the posture guarantees convergence back to the equilibrium. The local stability is

defined by the eigenvalues of the equilibrium. Similarly, the stability against small perturbations in walking is determined by the Floquet multipliers of the gait cycle, which Hurmuzlu et al. (1996) calculated from experimental data constructing a Poincaré map. Another method to assess local stability from experimental gait data is the calculation of maximum finite-time Lyapunov exponents (Dingwell and Cusumano 2000; Dingwell et al. 2000). Traditional measures of gait stability, based on kinematic variability, are poor predictors of local stability (Dingwell et al. 2001).

For both walking and posture tasks, the stability against larger perturbations is of great importance. In walking, for example, perturbations like tripping, stumbling, and pushing are frequent in daily life (Forner Cordero 2003). Stability against these kinds of perturbation cannot be determined by the calculation of the eigenvalues because for large perturbations linearization is in general not justified. In fact, for large perturbations the nonlinear terms of the differential equations determine the stability. Thus, local stability is only a necessary condition for stability against larger perturbations.

An interesting measure of stability is the *basin of attraction*. The basin of attraction of an attractor, such as a limit cycle, is the set of all the initial conditions in state space that lead to an orbit that approaches the attractor (Seydel 1988). Schwab and Wisse (2001) calculated the basin of attraction of the gait cycle of the simplest walking model for different slopes (i.e., different gravitational energy inputs). After comparison with the Floquet multipliers at these slopes, they concluded that there is no obvious relation between the local stability and the size of the basin of attraction. In other words, a better local stability margin does not imply a better stability margin against large perturbations.

The interpretation of the basin of attraction is easy in the above case because the basin of attraction equals all combinations of initial stance leg angles and angular velocities that lead to stable walking. If the basin of attraction is larger, the bipedal robot is easier to start up, and this is desirable. Thus, Schwab and Wisse (2001) concluded that the size of the basin of attraction is the most important stability measure in designing such bipedal robots. The question is if the basin of attraction is also a good measure of stability for human walking. In models of human walking, the basin of attraction can theoretically be computed in the same way as is done for the simplest walker, namely, by searching numerically the state space for all initial conditions under which the system returns to the cycle. However, more realistic models of walking can only be described by high-dimensional models, and this implies two problems. The first is the high computational effort required: the computation time for calculating the basin of attraction grows exponentially with system dimension, while the computation time for the 2D basin of the simplest walker is already long. The second problem is one of interpretation. Not only is the *size* of the basin of attraction given in terms of (hyper) volume of importance, but its shape is as well. If the basin of attraction increases substantially in some dimensions of

low importance but decreases a little in a very important dimension, looking only at the (hyper) volume of the basin leads to the wrong conclusion, namely, that the stability margin has increased. Another problem concerning the interpretation of the basin of attraction is that the states of the model are often an abstraction or simplification of reality and/or are not measurable (e.g., muscle activation). Thus for many states it is not known how much they are perturbed in real-life walking.

Stability in experimental gait studies is often quantified by indices, coming from rather intuitive tests, and have few predictive capabilities (Boulgarides et al. 2003). Moreover, the question remains whether the perturbations given in such tests are representative of those in everyday life. It would be useful to link the stability measures from theoretical and experimental research in the future to see how they are related and possibly to propose better ways of determining stability through experimental research.

#### 4.2 Concluding remarks

Bifurcation analysis was performed to show the influence of stretch reflexes, time delays, cocontraction, and force feedback on the behavior and stability of a model of stance. A fold and a Hopf branch divided the parameter space, in terms of muscle length and velocity feedback gains, into regions of different behavior: unstable posture, stable posture, and stable limit cycles. A linearized model was constructed and provides insight into the biomechanical causes for the bifurcations. The fold bifurcation represents zero ankle stiffness, below which the posture is unstable and a person falls. Ankle stiffness is increased by extra muscle length feedback, increased cocontraction, or positive force feedback. Feedback of muscle velocity is necessary to compensate for phase lag caused by time delay in the reflex arcs, muscle activation dynamics, and the presence of a compliant SE. The Hopf bifurcation represents the transition to unstable reflex loops. Beyond a Hopf bifurcation, for positive ankle stiffness the posture becomes unstable and a stable limit cycle emerges. The Hopf branch shrinks for increasing time delays, making the posture more susceptible to unstable reflex loops. Older people and people with injuries to the central nervous system often have larger time delays in their reflex arcs. The fact that these groups of people often have trouble with posture tasks such as standing might be explained by this increased time delay. Positive force feedback also reduces the size of the Hopf branch. More cocontraction leads to a growth of the Hopf branch, causing a larger region of postural stability in terms of stretch reflex gains. The period of the limit cycles, emerging beyond the Hopf branch, is mainly dependent on muscle length and velocity feedback and on the amount of time delay present in the reflex arc. The stable limit cycles do not correspond to the sway observed in human stance but rather to a neural deficiency termed ankle clonus. This is caused by higher effective reflex gains (i.e., reduced motoneuron firing threshold) together with the large time delay present in the reflex arcs of the ankles. A model fit to data of perturbed and quiet

stance in healthy subjects shows that stretch reflexes might be the major control mechanism in both cases.

This study has considered the influence of reflexes on stance by combining bifurcation analysis with more common biomechanical concepts and tools. It provides a framework for future research: we will develop this line of research to look at rhythmic tasks such as walking.

## References

- Amemiya M, Yamaguchi T (1984) Fictive locomotion of the forelimb evoked by stimulation of the mesencephalic locomotor region in the decerebrate cat. *Neurosci Lett* 50:91–96
- Arrowsmith DK, Place CM (1990) An introduction to dynamical systems. Cambridge University Press, Cambridge, UK, p 423
- Boulgarides LK, McGinty SM, Willett JA, Barnes CW (2003) Use of clinical and impairment-based tests to predict falls by community-dwelling older adults. *Phys Ther* 83:328–339
- Brown TG (1911) The intrinsic factors in the act of progression in the mammal. *Proc R Soc Lond B* 84:308–319
- Capaday C (2000) Control of a ‘simple’ stretch reflex in humans. *Trends Neurosci* 23:528–529
- Capaday C (2001) Force-feedback during human walking. *Trends Neurosci* 24:10
- Cohen AH, Wallen P (1980) The neuronal correlate of locomotion in fish. “Fictive swimming” induced in an *in vitro* preparation of the lamprey spinal cord. *Exp Brain Res* 41:11–18
- Dietz V (1998) Evidence for a load receptor contribution to the control of posture and locomotion. *Neurosci Biobehav Rev* 22:495–499
- Dietz V, Duysens J (2000) Significance of load receptor input during locomotion: a review. *Gait Posture* 11:102–110
- Dingwell JB, Cusumano JP (2000) Nonlinear time series analysis of normal and pathological human walking. *Chaos* 10: 848–863
- Dingwell JB, Cusumano JP, Sternad D, Cavanagh PR (2000) Slower speeds in patients with diabetic neuropathy lead to improved local dynamic stability of continuous overground walking. *J Biomech* 33:1269–1277
- Dingwell JB, Cusumano JP, Cavanagh PR, Sternad D (2001) Local dynamic stability versus kinematic variability of continuous overground and treadmill walking. *J Biomech Eng* 123:27–32
- Duysens J (2000) Reply. *Trends Neurosci* 23:529–530
- Duysens J, Van de Crommert HW (1998) Neural control of locomotion; The central pattern generator from cats to humans. *Gait Posture* 7:131–141
- Duysens J, Clarac F, Cruse H (2000) Load-regulating mechanisms in gait and posture: comparative aspects. *Physiol Rev* 80:83–133
- Engelborghs K, Luzyanina T, Samaey G (2001) DDE-BIF-TOOL v. 2.00: a Matlab package for bifurcation analysis of delay differential equations. In: Leuven KU (ed) Department of Computer Science, Heverlee, The Netherlands
- Fitzpatrick R, Rogers DK, McCloskey DI (1994) Stable human standing with lower-limb muscle afferents providing the only sensory input. *J Physiol* 480(Pt 2):395–403
- Forner Cordero A (2003) Human gait, stumble and ... fall? Mechanical limitations of the recovery from a stumble. Engineering technology. University of Twente, Enschede, The Netherlands, p 196
- Garcia M, Chatterjee A, Ruina A, Coleman M (1998) The simplest walking model: stability, complexity, and scaling. *J Biomech Eng* 120:281–288
- Grillner S, McClellan A, Perret C (1981) Entrainment of the spinal pattern generators for swimming by mechano-sensitive elements in the lamprey spinal cord *in vitro*. *Brain Res* 217:380–386
- Hidler JM, Rymer WZ (1999) A simulation study of reflex instability in spasticity: origins of clonus. *IEEE Trans Rehabil Eng* 7:327–340
- Hidler JM, Rymer WZ (2000) Limit cycle behavior in spasticity: analysis and evaluation. *IEEE Trans Biomed Eng* 47: 1565–1575
- Houk JC (1979) Regulation of stiffness by skeletomotor reflexes. *Annu Rev Physiol* 41:99–114
- Hurmuzlu Y, Basdogan C (1994) On the measurement of dynamic stability of human locomotion. *J Biomech Eng* 116:30–36
- Hurmuzlu Y, Basdogan C, Stoianovici D (1996) Kinematics and dynamic stability of the locomotion of post-polio patients. *J Biomech Eng* 118:405–411
- Inman V, Ralston H, Todd F (1981) Human Walking. Williams and Wilkins, Baltimore, MD
- Iooss G, Joseph DD (1990) Elementary stability and bifurcation theory. Springer, Berlin Heidelberg New York, p 324
- Kirsch RF, Rymer WZ (1987) Neural compensation for muscular fatigue: evidence for significant force regulation in man. *J Neurophysiol* 57:1893–1910
- Kuznetsov YA (1998) Elements of applied bifurcation theory. In: Marsden JE, Sirovich L (eds) Applied mathematical sciences vol 112. Springer, Berlin Heidelberg New York, p 591
- MacKay-Lyons M (2002) Central pattern generation of locomotion: a review of the evidence. *Phys Ther* 82:69–83
- Masani K, Popovic MR, Nakazawa K, Kouzaki M, Nozaki D (2003) Importance of body sway velocity information in controlling ankle extensor activities during quiet stance. *J Neurophysiol* 90:3774–3782
- McGeer T (1989) Powered flight, child’s play, silly wheels, and walking machines. In: Proceedings of the IEEE international conference on robotics and automation, Piscataway, NJ, pp 1592–1597
- McGeer T (1990) Passive dynamic walking. *Int J Robot Res* 9:62–82
- McMahon TA (1984) Muscles, reflexes, and locomotion. Princeton University Press, Princeton, NJ, p 331
- Mihelj M, Matjajic Z, Bajd T (2000) Postural activity of constrained subject in response to disturbance in sagittal plane. *Gait Posture* 12:94–104
- Morasso PG, Sanguineti V (2002) Ankle muscle stiffness alone cannot stabilize balance during quiet standing. *J Neurophysiol* 88:2157–2162
- Schwab AL, Wisse M (2001) Basin of attraction of the simplest walking model. In: Proceedings of ASME 2001 design engineering technical conferences and computers and information in engineering conference, Pittsburgh
- Seydel R (1988) From equilibrium to chaos: practical bifurcation and stability analysis. Elsevier, New York, p 367
- Sherwood L (1997) Human physiology: from cells to systems. Wadsworth, Belmont, p 753
- Shik ML, Severin FV, Orlovskii GN (1966) Control of walking and running by means of electrical stimulation of the mid-brain. *Biophysics* 11:756–765

- Sinkjaer T, Toft E, Andreassen S, Hornemann BC (1988) Muscle stiffness in human ankle dorsiflexors: intrinsic and reflex components. *J Neurophysiol* 60:1110–1121
- Taga G (1995a) A model of the neuro-musculo-skeletal system for human locomotion: I. Emergence of basic gait. *Biol Cybern* 73:97–111
- Taga G (1995b) A model of the neuro-musculo-skeletal system for human locomotion: II Real-time adaptability under various constraints. *Biol Cybern* 73:113–121
- Taga G (1998) A model of the neuro-musculo-skeletal system for anticipatory adjustment of human locomotion during obstacle avoidance. *Biol Cybern* 78:9–17
- Taga G, Yamaguchi Y, Shimizu H (1991) Self-organized control of bipedal locomotion by neural oscillators in unpredictable environment. *Biol Cybern* 65:147–159
- Thunnissen J (1993) Muscle force prediction during human gait. University of Twente, Den Haag, The Netherlands, p 221
- Van der Helm FC, Schouten AC, de Vlugt E, Brouwn GG (2002) Identification of intrinsic and reflexive components of human arm dynamics during postural control. *J Neurosci Meth* 119:1–14
- Van der Helm FCT, Rozendaal LA (2000) Musculoskeletal systems with intrinsic and proprioceptive feedback. In: Winters JM, Crago P (eds) *Neural control of posture and movement*. Springer, Berlin Heidelberg New York, pp 164–174
- Winter DA, Patla AE, Prince F, Ishac M, Gielo-Periczak K (1998) Stiffness control of balance in quiet standing. *J Neurophysiol* 80:1211–1221
- Winters JM, Stark L (1985) Analysis of fundamental human movement patterns through the use of in-depth antagonistic muscle models. *IEEE Trans Biomed Eng* 32:826–839
- Winters JM, Stark L (1987) Muscle models: what is gained and what is lost by varying model complexity. *Biol Cybern* 55:403–420
- Yamaguchi GT, Sawa AGU, Morgan DW, Fesler MJ, Winters JM (1990) A survey of human musculotendon actuator properties. In: Winters JM, Woo SL-Y (eds) *Multiple muscle systems: biomechanics and movement organization*. Springer, Berlin Heidelberg New York, pp 717–773
- Zehr EP, Stein RB (1999) What functions do reflexes serve during human locomotion? *Prog Neurobiol* 58:185–205

## Appendices

### Musculoskeletal model

*A Equations of motion.* The system contains six states: the activities of both muscles,  $a_{ta}$  and  $a_{sol}$ , the length of the CEs of both muscles,  $l_{ce,ta}$  and  $l_{ce,sol}$ , and the angle  $\theta$  and angular velocity  $\omega$  of the inverted pendulum.

Stretch reflexes are modeled by delayed feedback of the length of both muscles (relative to the rest lengths  $l_{m0}$ ),  $\Delta l_{mus,ta}$ , and  $\Delta l_{mus,sol}$ , and the velocities of both muscles,  $v_{mus,ta}$  and  $v_{mus,sol}$ . The lengths are fed back with gain  $k_p$  and the velocities with gain  $k_v$ . Force feedback is modeled as delayed feedback of muscle force with gain  $k_f$ .

A direct relation is assumed between the muscle lengths and velocities and the angle and angular velocity:

$$\begin{aligned} \Delta l_{mus,ta} &= -\theta \cdot r & \text{and} & & v_{mus,ta} &= -\omega \cdot r \\ \Delta l_{mus,sol} &= \theta \cdot r & \text{and} & & v_{mus,sol} &= \omega \cdot r \end{aligned}$$

Thus, reflexive feedback is modeled as delayed feedback of angle  $\theta(t - \tau)$ , angular velocity  $\omega(t - \tau)$ ,  $F_{se,ta}(t - \tau)$ , and  $F_{se,sol}(t - \tau)$ . The equations of motions are

$$\dot{a}_{ta} = \frac{1}{\tau_{ta}} \left( u_{ta} - a_{ta} - k_p c_{16} \theta(t - \tau) - k_v c_{16} \omega(t - \tau) + k_f F_{se,ta}(t - \tau) \right),$$

$$\dot{a}_{sol} = \frac{1}{\tau_{sol}} \left( u_{sol} - a_{sol} + k_p c_{16} \theta(t - \tau) + k_v c_{16} \omega(t - \tau) + k_f F_{se,sol}(t - \tau) \right),$$

$$\begin{aligned} \dot{l}_{ce,ta} &= c_4 v_{max,ta} \left( \frac{F v_{ce,ta} - 1}{F v_{ce,ta} + c_4} \right) \\ &\text{if } F v_{ce,ta} \leq 1 \quad (\text{contracting}), \end{aligned}$$

$$\begin{aligned} \dot{l}_{ce,ta} &= -c_6 v_{max,ta} \left( \frac{F v_{ce,ta} - 1}{F v_{ce,ta} - c_{17}} \right) \\ &\text{if } F v_{ce,ta} > 1 \quad (\text{lengthening}), \end{aligned}$$

$$\begin{aligned} \dot{l}_{ce,sol} &= c_4 v_{max,sol} \left( \frac{F v_{ce,sol} - 1}{F v_{ce,sol} + c_4} \right) \\ &\text{if } F v_{ce,sol} \leq 1 \quad (\text{contracting}), \end{aligned}$$

$$\begin{aligned} \dot{l}_{ce,sol} &= -c_6 v_{max,sol} \left( \frac{F v_{ce,sol} - 1}{F v_{ce,sol} - c_{17}} \right) \\ &\text{if } F v_{ce,sol} > 1 \quad (\text{lengthening}), \end{aligned}$$

$$\dot{\theta} = \omega,$$

$$\dot{\omega} = c_{11} M_p + c_{12} (F_{se,ta} - F_{se,sol}) + c_{13} \sin \theta,$$

in which the force-length relationships of CEs of the muscles are

$$\begin{aligned} Fl_{ce,ta} &= e^{-(c_2 l_{ce,ta} - c_3)^2}, \\ Fl_{ce,sol} &= e^{-(c_2 l_{ce,sol} - c_3)^2}, \end{aligned}$$

the nonlinear springs of the SEs of both muscles are

$$\begin{aligned} F_{se,ta} &= \min \left[ c_{10} a_{ta} Fl_{ce,ta}, c_7 \left( e^{c_8 (1 - c_1 - l_{ce,ta}) - c_9 \theta} - 1 \right) \right], \\ F_{se,sol} &= \min \left[ c_{10} a_{sol} Fl_{ce,sol}, c_7 \left( e^{c_8 (1 - c_1 - l_{ce,sol}) - c_9 \theta} - 1 \right) \right], \end{aligned}$$

the force-velocity relationships of the muscle are

$$\begin{aligned} F v_{ce,ta} &= \frac{F_{se,ta}}{c_5 a_{ta} Fl_{ce,ta}}, \\ F v_{ce,sol} &= \frac{F_{se,sol}}{c_5 a_{sol} Fl_{ce,sol}}, \end{aligned}$$

the maximum velocities of the muscles are

$$\begin{aligned} v_{max,ta} &= c_{14} \left( 1 - c_{15} \left( 1 - a_{ta} Fl_{ce,ta} \right) \right), \\ v_{max,sol} &= c_{14} \left( 1 - c_{15} \left( 1 - a_{sol} Fl_{ce,sol} \right) \right), \end{aligned}$$

and the activation and deactivation time constants of the muscle activation dynamics are

$$\tau_{ta} = \begin{cases} \tau_{ac} & \text{in case } a_{ta} \leq u_{ta} - k_p c_{16} \theta(t - \tau) - k_v c_{16} \\ & \quad \times \omega(t - \tau) + k_f F_{se,ta}(t - \tau) \\ \tau_{da} & \text{else } \tau_{ta} = \tau_{da}, \end{cases}$$

$$\tau_{\text{sol}} = \begin{cases} \tau_{\text{ac}} & \text{in case } a_{\text{sol}} \leq u_{\text{sol}} + k_p c_{16} \theta(t - \tau) + k_v \dot{c}_{16} \\ & \times \omega(t - \tau) + k_f F_{\text{se},\text{sol}}(t - \tau) \\ \tau_{\text{da}} & \text{else } \tau_{\text{sol}} = \tau_{\text{da}}. \end{cases}$$

Boundary conditions on certain states and functions are

$$\begin{aligned} 0 \leq a_{\text{ta}} \leq 1, & & 0 \leq a_{\text{sol}} \leq 1, \\ l_{\text{ce},\text{ta}} \geq 0, & & l_{\text{ce},\text{sol}} \geq 0, \\ F_{\text{se},\text{ta}} \geq 0, & & F_{\text{se},\text{sol}} \geq 0. \end{aligned}$$

Constants (all positive) used in the equations of motion above are dependent on muscle parameters in the following way:

$$\begin{aligned} c_1 &= \frac{l_t}{l_{m0}}, & c_2 &= \frac{1}{l_{\text{cesh}}}, \\ c_3 &= \frac{l_{\text{ce0}}}{l_{\text{cesh}}}, & c_4 &= m v_{\text{sh}}, \\ c_5 &= F_{\text{max}}, & c_6 &= m v_{\text{sh}} m v_{\text{sh}l}, \\ c_7 &= \frac{F_{\text{max}}}{e^{s e_{\text{sh}}} - 1}, & c_8 &= \frac{s e_{\text{sh}}}{s e_{\text{xm}}}, \\ c_9 &= \frac{r s e_{\text{sh}}}{l_{m0} s e_{\text{xm}}}, & c_{10} &= F_{\text{max}} \dot{m} v_{\text{ml}}, \\ c_{11} &= \frac{1}{I}, & c_{12} &= \frac{r}{I}, \\ c_{13} &= \frac{m g l_{\text{com}}}{I}, & c_{14} &= m v_{\text{vm}}, \\ c_{15} &= m v_{\text{er}}, & c_{16} &= r, \\ c_{17} &= (1 + m v_{\text{sh}} m v_{\text{sh}l}) (m v_{\text{ml}} - 1) + 1. \end{aligned}$$

The parameters have the following values and meaning:

$m = 80 \text{ kg}$	Mass of male person
$I = 121.6 \text{ kg m}^2$	Mass moment of inertia around ankles
$l_{\text{com}} = 1.0 \text{ m}$	Length between COM and ankles
$g = 9.81 \text{ m/s}^2$	Gravity constant
$r = 0.04 \text{ m}$	Moment arm about ankles
$l_{m0} = 0.305 \text{ m}$	Rest length of muscle
$l_t = 0.27 \text{ m}$	Tendon length
$l_{\text{ce0}} = 0.1$	Optimum length of CE (normalized on $l_{m0}$ )
$l_{\text{cesh}} = 0.03$	Shape parameter determining width of $F_{l_{\text{ce}}}$
$F_{\text{max}} = 8792 \text{ N}$	Maximum active muscle force
$m v_{\text{er}} = 0.5$	Scaling parameter for maximal contraction velocity
$m v_{\text{vm}} = 2 l_{m0}/s$	Maximal contraction velocity of unloaded CE
$m v_{\text{sh}} = 0.2$	Shape parameter of curvature of $F v_{\text{ce}}$
$m v_{\text{sh}l} = 0.5$	Shape parameter for lengthening curve of $F v_{\text{ce}}$
$m v_{\text{ml}} = 1.3$	Maximal force gain for lengthening muscles
$s e_{\text{sh}} = 4.4$	Shape parameter of curvature of exponential slope of SE
$s e_{\text{xm}} = 0.043$	Maximal extension of SE (normalized on $l_{m0}$ )
$\tau_{\text{ac}} = 11.33 \text{ ms}$	Time-constant for increased muscle activation
$\tau_{\text{da}} = 31.58 \text{ ms}$	Time-constant for decreasing muscle activation

**B Approximation of discontinuities.** The function  $F(x)$  is defined as:

$$F(x) = \begin{cases} -x & \text{if } x < 0, \\ x & \text{if } x \geq 0. \end{cases}$$

The function can be approximated by the following continuous function with the help of a hyperbolic tangent function as follows:

$$F_c(x) = x \tanh(SC x).$$

This way the discontinuities in the equations of motion (Appendix A) are *smoothed* into continuous functions for the performance of bifurcation analysis. The derivatives of the functions are also continuous.

The parameter SC represents the *steepness constant*. The higher SC is, the better the discontinuity is approached. The drawback is that a higher SC gives a stiffer system. SC is taken to be 1,000 in all the simulations.

**C Padé approximation of time delay.** For the linearized model discussed in Sect. 2.3, the time delay was modeled by a third-order Padé approximation. A Padé approximation of a time delay is based on a good approximation in the frequency domain. In the time domain the results will be less good. For the prediction of the eigenvalues associated with the equilibrium of the posture model of Sect. 2.1, a third-order Padé approximation gave good results (the higher the order, the better the approximation). The transfer function of the Padé approximation is as follows:

$$H_{\text{Padé}} = \frac{3 \tau^2 s^2 - 24 \tau s + 60}{\tau^3 s^3 + 9 \tau^2 s^2 + 36 \tau s + 60}.$$

To give an idea about the validity of the delay approximation, a comparison is made between the Padé approximation and the real delay in Laplace ( $H_\tau = e^{-j\omega\tau}$ ) with delay  $\tau = 50 \text{ ms}$ . This is shown in the Bode plot of Fig. 15.

The figure shows that the approximation in the frequency domain is good up to  $\omega_u = 50 \text{ [rad/s]}$ . This is much larger than the open-loop (i.e., before closing the reflex loop) bandwidth of the system. Therefore, depletion of the phase and gain margin, defining the transition of linear stability to linear instability, happens at frequencies much lower than the frequency up to which the Padé approximation is valid. Thus the approximation is at least valid up to the transition from linear stability to linear instability.

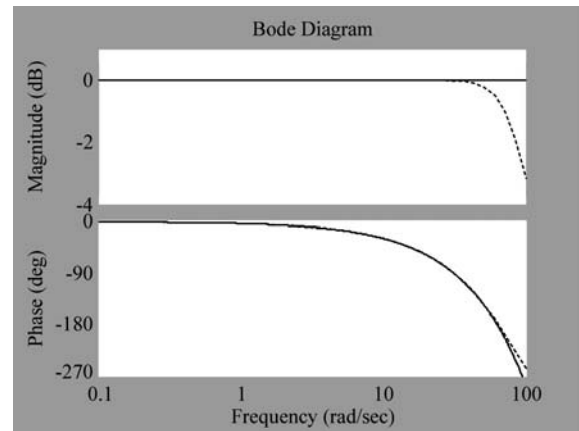


**Fig. 15.** Comparison of real delay of 50 ms (solid) and the third-order Padé approximation (dashed). The approximation is good up to 50 [rad/s]

Moreover, as long as the rightmost eigenvalues  $\lambda_{\text{rm}}$  of the system have an absolute value much smaller than the frequency  $\omega_u$  up to which the Padé approximation is valid (i.e.,  $|\lambda_{\text{rm}}| \ll \omega_u$ ), the prediction of the eigenvalues by the linearized model will also be quite good in the right half plane.

As an example, the eigenvalues were calculated for the equilibrium with parameter set  $[u \ k_p \ k_v \ k_f \ \tau]^T = [0.1 \ 1000 \ 10 \ 0 \ 50e-3]^T$ , thus way out of the stable area of

the parameter space (Fig. 4 in Sect. 3.1). The rightmost eigenvalues of the DDEs, calculated by DDE-BIFTOOL, are in this case  $\lambda_{\text{rm}} = 6.88 \pm 12.31i$ . The rightmost eigenvalues, predicted by the linearized model, are in this case  $\lambda_{\text{rm}} = 6.86 \pm 12.17i$ . Thus, while the absolute value of these eigenvalues, which is 14.1, is not *very* much lower than 50, it still gives a reasonably good approximation of the most dominant eigenvalues.